

Multiband superconductivity in $\text{PrPt}_4\text{Ge}_{12}$ single crystals

J. L. Zhang,¹ Y. Chen,¹ L. Jiao,¹ R. Gumeniuk,² M. Nicklas,² Y. H. Chen,¹ L. Yang,¹ B. H. Fu,¹ W. Schnelle,² H. Rosner,² A. Leithe-Jasper,² Y. Grin,² F. Steglich,² and H. Q. Yuan^{1,*}

¹*Department of Physics and Center for Correlated Matter,
Zhejiang University, Hangzhou, Zhejiang 310027, China*

²*Max-Planck-Institut für Chemische Physik fester Stoffe, Nöthnitzer Str. 40, 01187 Dresden, Germany*
(Dated: September 9, 2018)

We report measurements of the London penetration depth $\Delta\lambda(T)$ and the electronic specific heat $C_e(T)$ on high-quality single crystals of the filled-skutterudite superconductor $\text{PrPt}_4\text{Ge}_{12}$ ($T_c \simeq 8\text{K}$). Both quantities show a weak temperature dependence at $T \ll T_c$, following $\Delta\lambda \sim T^n$ ($n \simeq 3.2$) and $C_e/T \sim T^{2.8}$. Such temperature dependences deviate from both conventional s -wave type and nodal superconductivity. A detailed analysis indicates that the superfluid density $\rho_s(T)$, derived from the penetration depth, as well as the electronic specific heat can be consistently described in terms of a two-gap model, providing strong evidence of multiband superconductivity for $\text{PrPt}_4\text{Ge}_{12}$.

PACS numbers: 74.25.Bt; 74.20.Rp; 74.70.Dd; 74.70.Tx

The filled-skutterudite compounds MT_4X_{12} (M =rare-earth or alkaline-earth metals, T =Fe, Ru, Os, and X =P, As, Sb) demonstrate remarkably rich physical properties [1]. Particular attention has been paid to superconductivity (SC) observed in the Pr-based compounds. For example, $\text{PrOs}_4\text{Sb}_{12}$ is a heavy-fermion superconductor with $T_c = 1.85\text{ K}$ [2]. Electrical-quadrupole, rather than magnetic-dipole, fluctuations are believed to mediate the Cooper pairs in this compound, which is unique among heavy fermion superconductors. The superconducting order parameter of $\text{PrOs}_4\text{Sb}_{12}$ remains controversial: nodal SC [3, 4] as well as s -wave SC [5] were proposed. More recent experiments seem to support a scenario of multiband SC [6, 7]. On the other hand, the isostructural compounds $\text{PrRu}_4\text{Sb}_{12}$ and $\text{PrRu}_4\text{As}_{12}$ appear to be s -wave superconductors [8, 9].

Recently, a series of new skutterudite superconductors with a germanium-platinum framework, i.e., $M\text{Pt}_4\text{Ge}_{12}$ (M =Sr, Ba, La, Pr), were successfully synthesized [10, 11]. Among all the Pr-filled variants, $\text{PrPt}_4\text{Ge}_{12}$ shows an unexpectedly high transition temperature of $T_c=7.9\text{ K}$ [11]. The Sommerfeld coefficient of $\text{PrPt}_4\text{Ge}_{12}$ ($\gamma_n = 76\text{ mJ/mol K}^2$) [12] is comparable to that of $\text{PrRu}_4\text{Sb}_{12}$ [8] and $\text{PrRu}_4\text{As}_{12}$ [9], but much smaller than that of $\text{PrOs}_4\text{Sb}_{12}$ [2]. Furthermore, the crystalline electric field (CEF) splitting of the $J = 2$ Hund's rule multiplet of Pr^{3+} between the ground state and the first excited state is rather different among these Pr-based superconductors, e.g., $\Delta_{\text{CEF}} = 7\text{ K}$ for $\text{PrOs}_4\text{Sb}_{12}$ [13] and $\Delta_{\text{CEF}} = 130\text{ K}$ in $\text{PrPt}_4\text{Ge}_{12}$ [11, 14]. It is, therefore, of great interest to systematically compare the superconducting properties of these materials, which may help to elucidate their pairing mechanisms. Similar to $\text{PrOs}_4\text{Sb}_{12}$, previous studies on polycrystalline samples of $\text{PrPt}_4\text{Ge}_{12}$ showed controversial results. Measurements of the specific heat and muon-spin rotation (μSR) suggest the possible existence of point nodes in the superconducting gap [12]; zero-field μSR also provides evidence

of time reversal symmetry breaking below T_c [15], similar to what was observed for $\text{PrOs}_4\text{Sb}_{12}$ [16]. However, ^{73}Ge nuclear quadrupole resonance (NQR) experiments display a pronounced coherence peak in the spin-lattice relaxation rate $1/T_1$ at temperatures just below T_c , suggesting s -wave SC [17]. Very recently, a possible scenario of multiband SC was proposed for $\text{PrPt}_4\text{Ge}_{12}$, based on the analysis of the critical fields [18] as well as photoemission spectroscopy [19]. However, these experiments were performed on polycrystalline samples at relatively high temperatures, which could not make a clear assertion on the gap symmetry. The reasons underlying such discrepancies of the gap structure in $\text{PrPt}_4\text{Ge}_{12}$ are not yet clear, and further measurements, in particular those based on high-quality single crystals, are badly needed.

In this Letter, we probe the superconducting gap symmetry of $\text{PrPt}_4\text{Ge}_{12}$ by measuring the London penetration depth $\Delta\lambda(T)$ and the specific heat $C_p(T)$ of high-quality single crystals. Precise measurements of the penetration depth changes at low temperatures show $\Delta\lambda \sim T^n$ with $n \simeq 3.2$, indicating that $\text{PrPt}_4\text{Ge}_{12}$ is actually neither a simple BCS nor a nodal superconductor. A detailed analysis of the superfluid density $\rho_s(T)$, converted from $\lambda(T)$, and the electronic specific heat $C_e(T)$ provide strong evidence of two-band SC for $\text{PrPt}_4\text{Ge}_{12}$.

High-quality single crystals of $\text{PrPt}_4\text{Ge}_{12}$ were synthesized by using multi-step thermal treatments [20]. Powder X-ray diffraction indicates the presence of a small amount of foreign phases. Energy-dispersive X-ray (EDX) analysis confirms that all the crystals have a stoichiometric composition and the impurity phases, mainly PtGe_2 and free Ge, are located at the crystal surfaces [20]. In our measurements, the crystals were mechanically polished to get rid of these surface contaminations. Precise measurements of the resonant frequency shift $\Delta f(T)$ were performed by utilizing a tunnel diode oscillator (TDO) based, self-inductance method at an operating frequency of 7 MHz down to about 0.5K

in a ^3He cryostat [21]. The change of the penetration depth is proportional to the resonant frequency shift, i.e., $\Delta\lambda(T) = G\Delta f(T)$, where G is solely determined by the sample and coil geometries [4]. In this context, $\Delta\lambda(T)$ is extrapolated to zero at $T = 0$ by polynomial regression, i.e., $\Delta\lambda(T) = \lambda(T) - \lambda_0$. Here the value of zero-temperature penetration depth, $\lambda_0=114$ nm, was adopted from previous μSR experiments [12]. Measurements of the magnetic susceptibility were carried out in a SQUID magnetometer (Quantum Design), and the heat capacity was measured in a ^3He cryostat, using a relaxation method.

Figure 1 presents the electrical resistivity $\rho(T)$ for $\text{PrPt}_4\text{Ge}_{12}$, which shows an S-shape behavior upon cooling down from room temperature, as often observed in d -band materials. A sharp superconducting transition, evidenced from both the electrical resistivity $\rho(T)$ (inset (a)) and the magnetic susceptibility $\chi(T)$ (inset (b)), together with a large resistivity ratio ($\rho(300\text{K})/\rho(8\text{K})=19$) confirm the high quality of our single crystals. Furthermore, the superconducting transition temperatures T_c , determined from the zero resistivity and the onset of the magnetic susceptibility, are nearly the same ($T_c \simeq 7.8$ K), proving good homogeneity of the samples.

The inset of Fig. 2 shows the change of the penetration depth $\Delta\lambda(T)$ up to 9K, which reveals a sharp superconducting transition at $T_c \simeq 8.1$ K. Here $G=2.13\text{\AA}/\text{Hz}$. It is noted that we have measured the penetration depth for several samples and the data are well reproducible. The values of T_c , derived for different samples by distinct methods, are nearly same too. In the main plot of Fig. 2, we presents $\Delta\lambda(T)$ at low temperatures, together with the fits of various models to the data. Obviously, the standard BCS model can not describe the experi-

mental data. Moreover, the penetration depth $\Delta\lambda(T)$ deviates also from that of nodal SC, for which a linear and quadratic temperature dependence is expected for the case of line and point nodes, respectively. Instead, a power law of $\Delta\lambda \sim T^n$ ($n \simeq 3.2$) presents a reasonable fit to the experimental data. An enhanced power-law exponent n , e.g., a quadratic temperature dependence in d -wave superconductors, may arise from nonlocal effects or impurity scattering [22]. However, such possibilities are excluded for $\text{PrPt}_4\text{Ge}_{12}$ because both the penetration depth ($\lambda_0 = 114$ nm) [12] and the mean free path ($l = 103$ nm) are much larger than the coherence length ($\xi_0 = 13.5$ nm) [12], implying that the samples are in the clean and local limit. Here we estimate the mean free path from $l = [\frac{\xi_0^{-2} - 1.6 \times 10^{12} \rho_0 \gamma_n T_c}{1.8 \times 10^{24} (\rho_0 \gamma_n T_c)^2}]^{1/2}$ [23], where ρ_0 , ξ_0 and γ_n represent the electrical resistivity at $T_c=7.8\text{K}$ ($\rho_0 = 3.5 \times 10^{-6} \Omega\text{cm}$), the aforementioned coherence length and the Sommerfeld coefficient at T_c ($\gamma_n = 1795 \text{ erg cm}^{-3}\text{K}^{-2}$), respectively. On the other hand, multi-band effects may also give rise to power-law-like behavior at low temperatures with a large exponent n , which will be further elucidated by the analysis of both the superfluid density and specific heat.

The superfluid density $\rho_s(T)$ provides an important characterization of the superconducting gap symmetry. Fig. 3 shows the temperature dependence of the normalized superfluid density $\rho_s(T)$ for $\text{PrPt}_4\text{Ge}_{12}$ (circles), which is calculated by $\rho_s = [\lambda_0/\lambda(T)]^2$. For comparison, in Fig.3 we also include the superfluid density from the μSR results determined on polycrystalline samples (diamonds) [12]. Obviously, these two data sets are quite compatible, although the μSR data are more scattered, with a poor resolution when compared with the

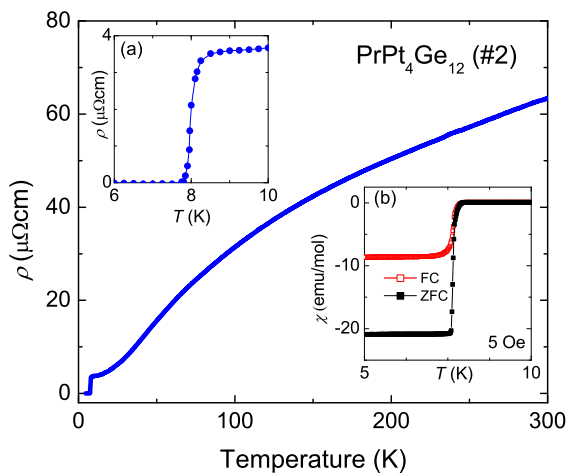


FIG. 1: Temperature dependence of the electrical resistivity $\rho(T)$ for $\text{PrPt}_4\text{Ge}_{12}$. Insets show the superconducting transitions in the electrical resistivity $\rho(T)$ (a) and magnetic susceptibility $\chi(T)$ (b), respectively.

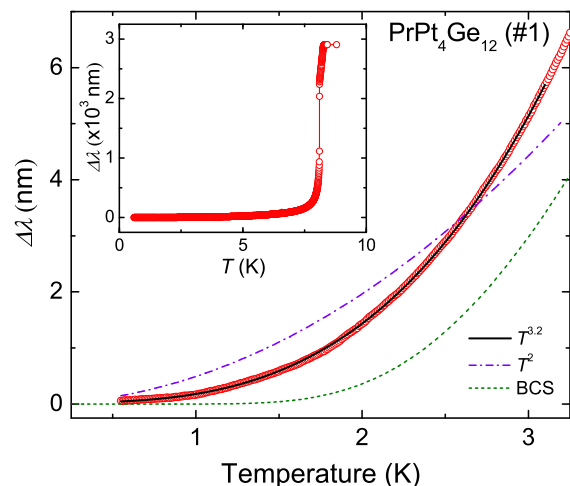


FIG. 2: Temperature dependence of the penetration depth $\Delta\lambda(T)$ for $\text{PrPt}_4\text{Ge}_{12}$. Solid, dash-dotted and dashed lines represent the fit of $\Delta\lambda \sim T^{3.2}$, $\Delta\lambda \sim T^2$ (point node) and single-gap BCS model, respectively. Inset shows $\Delta\lambda(T)$ over the entire temperature range.

TDO results. This allows to probe the gap structure of PrPt₄Ge₁₂ in a much more precise way than before.

The superfluid density can be calculated by:

$$\rho_s(T) = 1 + 2 \left\langle \int_0^\infty \frac{\partial f}{\partial E} \frac{E}{\sqrt{E^2 - \Delta_k^2(T)}} dE \right\rangle_{\text{FS}}, \quad (1)$$

where $f = (e^{\sqrt{E^2 + \Delta_k^2(T)}/k_B T} + 1)^{-1}$ is the Fermi distribution function and $\langle \dots \rangle_{\text{FS}}$ denotes the average over the Fermi surface. For the temperature dependence of the energy gap, we take $\Delta(T) = \Delta_0 \tanh \frac{\pi k_B T_c}{\Delta_0} \left[\frac{2}{3} \frac{\Delta C_e}{\gamma_n T_c} \left(\frac{T}{T_c} - 1 \right) \right]^{0.5}$ [24]. Here ΔC_e is the specific heat jump at T_c . Note that Eq. 1 is applicable for various gap functions $\Delta_k (= \Delta(\theta, \phi))$ in the pure/local limit. Given a gap function $\Delta(\theta, \phi)$, then one can fit it to the experimental data. Here θ and ϕ denote the angles away from the z-axis and x-axis in k-space, respectively. In this analysis, the zero-temperature gap amplitude, Δ_0 , is the sole fitting parameter.

Possible symmetries of the order parameter have been theoretically investigated for the skutterudite superconductors with tetrahedral point group symmetry (T_h) [25]. Various gap functions $\Delta(\theta, \phi)$, restrained by the crystal symmetry, have been adopted to fit the superfluid density $\rho_s(T)$ of PrOs₄Sb₁₂ [4]. In this context, we apply a similar analysis to the experimentally obtained $\rho_s(T)$ data of PrPt₄Ge₁₂. Fig. 3 presents the fits of different gap functions allowed by the crystal symmetry; the derived fitting parameters of Δ_0 are summarized in Table 1. Apparently, the gap functions B and E cannot reproduce the experimental data. On the other hand, the fits of functions A, C and D are close to the experimental data, but show significant deviations at low temperatures (inset of Fig.3). We note that models C and D, both hav-

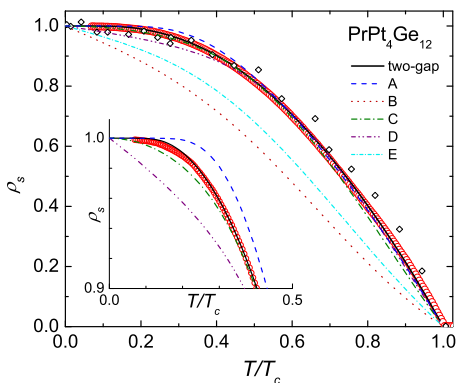


FIG. 3: Superfluid density $\rho_s(T)$ versus normalized temperature T/T_c . Inset expands the low temperature region. Circle (○) and diamond (◇) display the experimental data derived from TDO measurements (this study) and μ SR experiments (from Ref.[12]), respectively. Lines shows theoretical fits of various gap functions as listed in Table 1.

TABLE I: Summary of various gap functions and so derived fitting parameters Δ_0 .

model	Gap function $\Delta(\theta, \phi)$	$\Delta_0/k_B T_c$
A	Δ_0	1.76
B	$ \Delta_0 \sin \theta \sin \phi $	4
C	$ \Delta_0 \sin \theta $	2.7
D	$\Delta_0(1 - \sin^4 \theta \cos^4 \theta)$	2.9
E	$\Delta_0(1 - (\sin^4 \phi + \cos^4 \phi) \sin^4 \theta)$	3.2

ing point nodes in the superconducting gap, were previously assumed to present a good fit to the μ SR data [15], which are rather scattered at low temperature. The more precise measurements of the penetration depth, $\Delta\lambda(T)$, and the corresponding superfluid density, $\rho_s(T)$, indicate that the conventional one-gap BCS model as well as the nodal-gap model D provide a poor fit to the low temperature data. The nodal-gap model C can fit the TDO data relatively well, but significant deviations remain below $0.4T/T_c$. Instead, the two-gap BCS model gives the best fit to our experimental data.

In the case of two-gap BCS superconductors, the superfluid density can be extended to the following linear combination[26]:

$$\tilde{\rho}_s(T) = x\rho_s(\Delta_0^1, T) + (1-x)\rho_s(\Delta_0^2, T), \quad (2)$$

where $\Delta_0^i (i = 1, 2)$ represent the size of two isotropic gaps at zero temperature, and x is the relative weight of the contributions from Δ_0^1 . As shown in Fig. 3, the two-gap BCS model nicely fits the experimental data of PrPt₄Ge₁₂ over the entire temperature region. The so derived parameters of $\Delta_0^1 = 0.8k_B T_c$, $\Delta_0^2 = 2.0k_B T_c$ and $x=0.15$ meet the theoretical constraints that one gap is larger than the BCS value and the other one is smaller [27], as demonstrated in the prototype two-gap BCS superconductor MgB₂ [26].

In Fig. 4, we present the low-temperature specific heat, $C_p(T)$, of a PrPt₄Ge₁₂ single crystal. A sharp superconducting transition is observed at $T_c = 7.7$ K, being close to that determined from other experiments. The specific heat data above T_c can be fitted by a polynomial expansion $C_p(T) = \gamma_n T + \beta T^3$. Here $C_e = \gamma_n T$ and $C_{ph} = \beta T^3$ denote the electronic and phonon contributions, respectively. This yields the Sommerfeld coefficient in the normal state, $\gamma_n = 69$ mJ/mol K², and the Debye temperature $\Theta_D = 190$ K, which are close to those found in case of polycrystalline samples [12]. For polycrystals [12], a pronounced upturn was previously reported in the low-temperature specific heat $C_e(T)/T$. Similar specific heat anomalies were also observed in some as-grown single crystals. A careful examination showed that such an upturn in $C_e(T)/T$ has to be attributed to a nuclear Schottky anomaly caused by the Pr-containing surface contaminations [20]. Indeed, the specific heat anomaly disappears for the polished single crystal as shown in Fig.4(b), allowing us to accurately analyze its low tem-

perature behavior.

The electronic specific heat of $\text{PrPt}_4\text{Ge}_{12}$, obtained after subtracting the phonon contributions, is presented in the main part and inset (b) of Fig. 4 as C_e/T versus T , together with the fits of various models. As shown in the inset (b), the data can be well described by a power law, $C_e/T \sim T^{2.8}$. This behavior deviates from the quadratic temperature dependence of $C_e(T)/T$ reported in Ref. [12]. The discrepancy is likely to result from the nuclear Schottky anomaly of the polycrystalline samples discussed before. With the previous data [12], a proper subtraction of this Schottky anomaly is difficult and, therefore, deviations from the true specific-heat behavior become likely at low temperatures. Furthermore, the standard BCS-model is not sufficient to fit the experimental data (Fig. 4(b)), while the two-gap BCS model presents the best fit to the $C_e(T)/T$ data (main figure). According to the phenomenological two-gap BCS model, the heat capacity is taken as the sum of contributions from the two bands, each one following the BCS-type temperature dependence [28]. In the main panel of Fig. 4, we plot the contributions from the two superconducting gaps, $\Delta_0^1 = 0.8k_B T_c$ and $\Delta_0^2 = 2.0k_B T_c$, as well as their sum (solid line). The weight contributed from the first gap, Δ_0^1 , is $x=0.12$. All these fitting parameters are remarkably consistent with those obtained from the superfluid density $\rho_s(T)$, providing strong evidence of two-gap SC for $\text{PrPt}_4\text{Ge}_{12}$.

Evidence of BCS-like SC, including two-gap type, has been observed in several skutterudite compounds. For

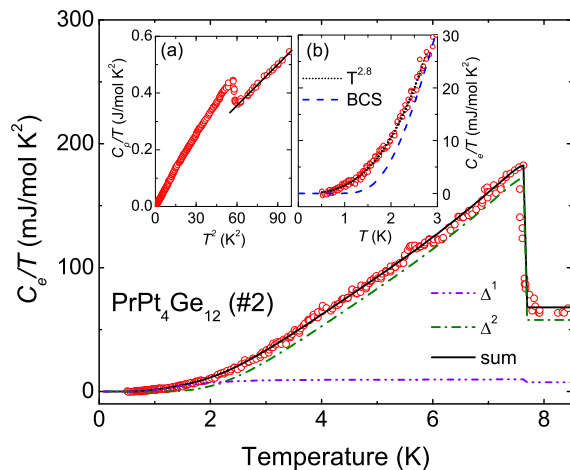


FIG. 4: Temperature dependence of the electronic specific heat $C_e(T)/T$ of a $\text{PrPt}_4\text{Ge}_{12}$ single crystal at zero field. Dash dotted lines (green and blue) and solid line show the individual and total contributions of the two gaps to the specific heat $C_e(T)/T$, respectively. Inset (a): total specific heat, $C_p(T)/T$, plotted as a function of T^2 . Inset (b): electronic specific heat $C_e(T)/T$ at low temperatures, fitted by $C_e/T \sim T^{2.8}$ (dotted line). Dashed line refers to the standard BCS model.

example, $\text{PrRu}_4\text{Sb}_{12}$ [8], $\text{PrRu}_4\text{As}_{12}$ [9] and their non- $4f$ counterparts [12] are believed to be s -wave superconductors. Recent measurements indicate that $\text{PrOs}_4\text{Sb}_{12}$ is an extreme two-band superconductor [6, 7]; here energy nodes were assumed to exist in the small gap, and the isotropic large gap dominates the superconducting properties near T_c [7], or when a sufficiently large magnetic field is applied [29]. Two-gap BCS SC was also proposed for both $\text{PrRu}_4\text{Sb}_{12}$ [7] and $\text{LaOs}_4\text{Sb}_{12}$ [30], the latter one suggesting that $4f$ -electrons are not the origin of multiband SC. In $\text{PrPt}_4\text{Ge}_{12}$, band structure calculations indicate an only minor contribution of the $4f$ -electrons to the density of states at the Fermi energy, suggesting that the $4f$ -electrons may not be playing a significant role on SC in this compound either [11]. Indeed, the thermodynamic properties and low-lying CEF scheme of $\text{PrPt}_4\text{Ge}_{12}$ seem to be rather different from those of the heavy fermion compound $\text{PrOs}_4\text{Sb}_{12}$, but resemble other skutterudite compounds [8, 9]. Indications of two-gap SC for $\text{PrPt}_4\text{Ge}_{12}$ were also inferred from recent measurements of the upper and lower critical fields [18] and photoemission spectroscopy [19]. Furthermore, multiband SC is compatible with the observations of a coherence peak in the NQR measurements just below T_c [17]. Such a multi-gap structure seems to be characteristic for the skutterudite superconductors; the small gap, either with or without nodes, is rather subtle and can be easily destroyed by external effects, e.g., a magnetic field, so that the large gap is predominant. Recent μSR measurements performed on polycrystalline samples of $\text{PrPt}_4\text{Ge}_{12}$ showed evidence of time-reversal symmetry breaking [15]. To confirm it and check the possible existence of nodes in the small gap of $\text{PrPt}_4\text{Ge}_{12}$, it would be important to repeat these measurements with high-quality single crystals. Detailed calculations of its electronic structure are also highly desirable in order to further elucidate the multiband structure in $\text{PrPt}_4\text{Ge}_{12}$. Moreover, comparative studies of the Pr-based skutterudites and the non- f electron isostructural compounds, e.g., $M\text{Pt}_4\text{Ge}_{12}$ ($M = \text{Sr}, \text{Ba}$ and La), are necessary to reveal the potential role of f -electrons on SC.

In summary, we have studied the superconducting order parameter of $\text{PrPt}_4\text{Ge}_{12}$ by measuring the penetration depth $\Delta\lambda(T)$ and specific heat $C_p(T)$ on high-quality single crystals. For $T \ll T_c$, both quantities demonstrate a weak temperature dependence and can be fitted by a power-law behavior with a large exponent, i.e., $\Delta\lambda \sim T^{3.2}$ and $C_e/T \sim T^{2.8}$, which is inconsistent with both a single-gap BCS model and nodal-gap SC. Instead, we can describe the superfluid density $\rho_s(T)$ and the electronic specific heat $C_e(T)$ in terms of a phenomenological two-gap BCS model with consistent gap parameters of $\Delta_0^1 = 0.8k_B T_c$, $\Delta_0^2 = 2.0k_B T_c$ and $x = 0.12 \sim 0.15$, the weight contributed by the small gap. These findings have elucidated the controversial results found in the literature and provide unambiguous evidence of multiband

SC for PrPt₄Ge₁₂.

We are grateful to E. Rosseeva, Y. Kohama and C. T. van Degrift for providing experimental assistance. This work was supported by the National Basic Research Program of China (NOs. 2009CB929104 and 2011CBA00103), NSFC (NOs. 10934005 and 11174245), Zhejiang Provincial Natural Science Foundation of China, the Fundamental Research Funds for the Central Universities and the Max-Planck Society under the auspices of the Max-Planck Partner Group of the MPI for Chemical Physics of Solids, Dresden.

* Electronic address: hqyuan@zju.edu.cn

- [1] B. C. Sales, Handbook on the Physics and Chemistry of Rare Earths, edited by K. A. Gschneidner, Jr., J.-C. G. Bünzli, and V.K. Pecharsky (Elsevier, Amsterdam, 2003), Vol. 33, p. 1.
- [2] E. D. Bauer, N. A. Frederick, P.-C. Ho, V. S. Zapf, and M. B. Maple, Phys. Rev. B 65, 100506(R) (2002).
- [3] K. Izawa, Y. Nakajima, J. Goryo, Y. Matsuda, S. Osaki, H. Sugawara, H. Sato, P. Thalmeier, and K. Maki, Phys. Rev. Lett. 90, 117001 (2003).
- [4] E. E. M. Chia, M. B. Salamon, H. Sugawara, and H. Sato, Phys. Rev. Lett. 91, 247003 (2003), and references therein.
- [5] D. E. MacLaughlin, J. E. Sonier, R. H. Heffner, O. O. Bernal, B. L. Young, M. S. Rose, G. D. Morris, E. D. Bauer, T. D. Do, and M. B. Maple, Phys. Rev. Lett. 89, 157001 (2002).
- [6] G. Seyfarth, J. P. Brison, M.-A. Méasson, D. Braithwaite, G. Lapertot, and J. Flouquet, Phys. Rev. Lett. 97, 236403 (2006).
- [7] R. W. Hill, S. Y. Li, M. B. Maple, and L. Taillefer, Phys. Rev. Lett. 101, 237005 (2008).
- [8] N. Takeda and M. Ishikawa, J. Phys. Soc. Jpn. 69, 868 (2000).
- [9] T. Namiki, Y. Aoki, H. Sato, C. Sekine, I. Shirogami, T. D. Matsuda, Y. Haga, and T. Yagi, J. Phys. Soc. Jpn. 76, 093704 (2007).
- [10] E. Bauer et al., Phys. Rev. Lett. 99, 217001 (2007).
- [11] R. Gumeniuk, W. Schnelle, H. Rosner, M. Nicklas, A. Leithe-Jasper, and Y. Grin, Phys. Rev. Lett. 100, 017002 (2008).
- [12] A. Maisuradze, M. Nicklas, R. Gumeniuk, C. Baines, W. Schnelle, H. Rosner, A. Leithe-Jasper, Y. Grin, and R. Khasanov, Phys. Rev. Lett. 103, 147002 (2009).
- [13] M. B. Maple, N.A. Frederick, P.-C. Ho, W. M. Yuhasz, and T. Yanagisawa, J. Supercond. Novel Magnetism 19, 229 (2006).
- [14] M. Toda, H. Sugawara, K. Magishi, T. Saito, K. Koyama, Y. Aoki, and H. Sato, J. Phys. Soc. Jpn. 77, 124702 (2008).
- [15] A. Maisuradze, W. Schnelle, R. Khasanov, R. Gumeniuk, M. Nicklas, H. Rosner, A. Leithe-Jasper, Y. Grin, A. Amato, and P. Thalmeier, Phys. Rev. B 82, 024524 (2010).
- [16] Y. Aoki et al., Phys. Rev. Lett. 91, 067003 (2003).
- [17] F. Kanetake, H. Mukuda, Y. Kitaoka, K. Magishi, H. Sugawara, K. M. Itoh, and E. E. Haller, J. Phys. Soc. Jpn. 79, 063702 (2010).
- [18] L. S. Sharath Chandra, M. K. Chattopadhyay, and S. B. Roy, Phil. Mag. DOI:10.1080/14786435.2012.691218 (2012).
- [19] Y. Nakamura, H. Okazaki, R. Yoshida, T. Wakita, H. Takeya, K. Hirata, N. Hirai, Y. Muraoka, and T. Yokoya, Phys. Rev. B 86, 014521 (2012).
- [20] See Supplementary Materials for sample preparations and characterizations.
- [21] C. T. Van Degrift, Rev. Sci. Instrum. 46, 599 (1975).
- [22] P. J. Hirschfeld and N. Goldenfeld, Phys. Rev. B 48, 4219 (1993)
- [23] T. P. Orlando, E. J. McNiff Jr., S. Foner and M. R. Beasley, Phys. Rev. B 19, 4545 (1979)
- [24] R. Prozorov and R. W. Giannetta, Supercond. Sci. Technol. 19, R41 (2006).
- [25] I. A. Sergienko and S. H. Curnoe, Phys. Rev. B 70, 144522 (2004).
- [26] F. Manzano, A. Carrington, N.E. Hussey, S. Lee, A. Yamamoto, and S. Tajima, Phys. Rev. Lett. 88, 047002 (2002).
- [27] V. Z. Kresin and S. A. Wolf, Physica C 169, 476 (1990).
- [28] F. Bouquet, Y. Wang, R. A. Fisher, D. G. Hinks, J. D. Jorgensen, A. Junod, and N. E. Phillips, Europhys. Lett. 56, 856 (2001).
- [29] L. Shu, D. E. MacLaughlin, W. P. Beyermann, R. H. Heffner, G. D. Morris, O. O. Bernal, F. D. Callaghan, J. E. Sonier, W. M. Yuhasz, N. A. Frederick, and M. B. Maple, Phys. Rev. B 79, 174511 (2002).
- [30] X. Y. Tee, H. G. Luo, T. Xiang, D. Vandervelde, M. B. Salamon, H. Sugawara, H. Sato, C. Panagopoulos, and E. E. M. Chia, Phys. Rev. B 86, 064518 (2012).